AD736483

# FOREIGN TECHNOLOGY DIVISION

THE STUDY OF PLASMA FORMED BY
ULTRASHORT LASER PULSES
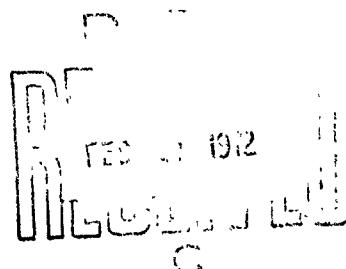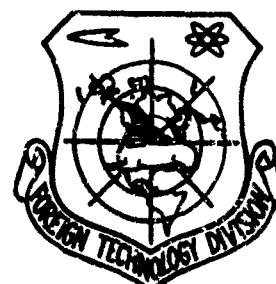
by

N. G. Basov, S. D. Zakharov, et al.

DOCUMENT CONTROL DATA - R & D

(Security classification of title, body of abstract and indexing annotation must be entered when the overall report is classified)

1. ORIGINATING ACTIVITY (Corporate author)	2a. REPORT SECURITY CLASSIFICATION
Foreign Technology Division Air Force Systems Command U. S. Air Force	UNCLASSIFIED
	2b. GROUP

3. REPORT TITLE

THE STUDY OF PLASMA FORMED BY ULTRASHORT LASER PULSES

4. DESCRIPTIVE NOTES (Type of report and inclusive dates)

Translation

5. AUTHOR(S) (First name, middle initial, last name)

Basov, N. G.; Zakharov, S. D.; Krohkin, O. N.; Kryukov, P. G.; Senatskiy, Yu. V.

6. REPORT DATE	7a. TOTAL NO. OF PAGES	7b. NO. OF REFS
1971	44	

8a. CONTRACT OR GRANT NO.	9a. ORIGINATOR'S REPORT NUMBER(S)
b. PROJECT NO. AAKM	FTD-MT-24-987-71
c.	9b. OTHER REPORT NO(S) (Any other numbers that may be assigned this report)
d. DIA Task No. T65-05-32	

10. DISTRIBUTION STATEMENT

Approved for public release; distribution unlimited.

11. SUPPLEMENTARY NOTES	12. SPONSORING MILITARY ACTIVITY
	Foreign Technology Divison Wright-Patterson AFB, Ohio

13. ABSTRACT

Processes occurring during high-temperature heating of plasma have been studied experimentally by focusing laser emission of ultrashort duration on the surface of lithium deuteride. Experiments included the shadow photography of plasma with illumination by ultrashort pulses and the photo-registration of the dispersion of plasma with the aid of an image inverter, as well as the time dependence of laser pulse reflection and the measurement of the electron temperature of plasma with respect to its X-ray radiation. The basic processes which accompany the heating of plasma by ultrashort pulses are examined theoretically within the framework of approximations based upon the results of experiments.

DD FORM 1473
I NOV 65

KEY WORDS	LINK A		LINK B		LINK	
	ROLE	WT	ROLE	WT	ROLE	WT
Laser Pulse						
Ultrashort Laser						
Laser Optics						
Pulse Length						

EDITED MACHINE TRANSLATION

THE STUDY OF PLASMA FORMED BY ULTRASHORT LASER PULSES

By: N. G. Basov, S. D. Zakharov, et al.

English pages: 44

Source: Kvantovaya Elektronika (Quantum Electronics), No. 1, 1971, 29 pages.

This document is a Systran machine aided translation, post-edited for technical accuracy by: Louise Heenan

Approved for public release; distribution unlimited.

PREPARED BY:

TRANSLATION DIVISION
FOREIGN TECHNOLOGY DIVISION
WP-AFB, OHIO.

Date 11 Nov 19 71

U. S. BOARD ON GEOGRAPHIC NAMES TRANSLITERATION SYSTEM

Block	Italic	Transliteration	Block	Italic	Transliteration
А а	*А а*	A, a	Р р	*Р р*	R, r
Б б	*Б б*	B, b	С с	*С с*	S, s
В в	*В в*	V, v	Т т	*Т т*	T, t
Г г	*Г г*	G, g	У у	*У у*	U, u
Д д	*Д д*	D, d	Ф ф	*Ф ф*	F, f
Е е	*Е е*	Ye, ye; E, e*	Х х	*Х х*	Kh, kh
Ж ж	*Ж ж*	Zh, zh	Ц ц	*Ц ц*	Ts, ts
З з	*З з*	Z, z	Ч ч	*Ч ч*	Ch, ch
И и	*И и*	I, i	Ш ш	*Ш ш*	Sh, sh
Й й	*Й й*	Y, y	Щ щ	*Щ щ*	Shch, shch
К к	*К к*	K, k	Ъ ъ	*Ъ ъ*	"
Л л	*Л л*	L, l	Ы ы	*Ы ы*	Y, y
М м	*М м*	M, m	Ь ь	*Ь ь*	'
Н н	*Н н*	N, n	Э э	*Э э*	E, e
О о	*О о*	O, o	Ю ю	*Ю ю*	Yu, yu
П п	*П п*	P, p	Я я	*Я я*	Ya, ya

* ye initially, after vowels, and after ъ, ь; e elsewhere.
When written as ё in Russian, transliterate as yё or ё.
The use of diacritical marks is preferred, but such marks
may be omitted when expediency dictates.

THE STUDY OF PLASMA FORMED BY ULTRA-
SHORT LASER PULSES

N. G. Basov, S. D. Zakharov, O. N.
Krokhin, P. G. Kryukov, Yu. V.
Senatskiy, Ye. L. Tyurin, A. I.
Fedosimov, S. V. Chekalin, and
M. Ya. Shchelev

     Processes occurring during high-temperature
heating of plasma have been studied experimentally
by focusing laser emission of ultrashort duration
on the surface of lithium deuteride. Experiments
included the shadow photography of plasma with
illumination by ultrashort pulses and the photo-
registration of the dispersion of plasma with the
aid of an image inverter, as well as the time
dependence of laser pulse reflection and the
measurement of the electron temperature of plasma
with respect to its X-ray radiation.

     The basic processes which accompany the
heating of plasma by ultrashort pulses are
examined theoretically within the framework of
approximations based upon the results of experi-
ments.

I. Introduction

  In 1968 in the Quantum Radiophysics Laboratory of the Physics
Institute imeni P. N. Lebedev of the Academy of Sciences USSR,
research was started on the heating of plasma by laser emission of
ultrashort duration (10^{-11}-10^{-12} s). Upon focusing such pulses to
the surface of a target of lithium deuteride placed in vacuum, it
was possible to register rapid neutrons [1]. This fact indicated

the existence of conditions of thermonuclear d-d-reaction and, consequently, the achievement of high values of temperature and density in the plasma. Thus it was shown that the energy of a powerful laser of ultrashort duration can be effectively introduced in the plasma.

At the same time it was established that the significant part of the laser emission is reflected from the target [1, 2]. These results were confirmed in references [3, 4].

In the analysis of the findings a number of questions appear. In the first place, in what manner does energy absorption by a solid body occur if the laser emission has been concentrated in a pulse of several picoseconds duration? In the second place, how do we explain the power reflection of laser emission from the target? And finally, what are the possibilities of ion temperature increase and, consequently, neutron yield during the heating of plasma by ultrashort pulses?

To answer these questions supplementary experiments were made which investigated the basic features of heating and dispersion in the plasma being formed. Some of them have been described in reference [5].

Furthermore, it was established with the aid of the high-resolution photoregistering apparatus that structure of the laser emission pulse has a complex character and is not reproduced from experiment to experiment.

The ability of the plasma volume to generate thermonuclear neutrons is determined by the values of temperature, density, and lifetime for the plasma in this volume. In the plasma formed by ultrashort laser pulses, these parameters are changed depending upon time as well as upon coordinates, whereupon the characteristic time of dispersion is $\sim 10^{-9}$ s and the characteristic dimension is $\sim 10^{-2}$ cm. Therefore, the registration of plasma parameters with simultaneous space and time resolutions ($\Delta x \approx 10^{-3}$ cm, $\Delta t \sim 10^{-10}$ s) is a difficult

technical problem, which is even more complicated due to the non-reproducibility of laser pulses from burst to burst [2]. Nevertheless, the achievement of either space or time resolution individually is possible in practice. In this work we selected an alternate plan, i.e., in our experiments we recorded parameters with high time resolution (to $2 \cdot 10^{-11}$ s) averaged by the plasma volume. In this case, we attempted to check the results of one procedure by the data obtained with another. The measurements, whose results are examined later, were made with total pulse energy 0.1 J. We used smaller fluxes than in [1] becuase of the working conditions of the laser; for more detail see [5]. Lithium deuteride LiD was used as a target.

Theoretical research on the possibilities of heating ions by focusing ultrashort pulses on a solid target is of considerable interest. A physical model of heating was constructed with the aid of experimental data. Calculation was performed within the framework of hydrodynamic equations of two-component plasma, averaged with respect to space, taking into account electron-ion relaxation and energy losses to emissions when the duration of laser pulse is considerably shorter than the characteristic plasma time (relaxation time, time of hydrodynamic dispersion). This makes it possible to examine processes in plasma from the moment of the termination of laser pulse, selecting as boundary conditions the parameters of plasma n_0, x_0, T_0 which is formed after ultrashort pulses (n_0 — electron density, x_0 — characteristic dimension, T_0 — electron temperature). With the aid of such an approximation model, the analytical dependence of maximum ion temperature on the initial parameters, which can be measured experimentally, has been found. The simplifications made in the calculation, consisting of the arbitrariness of n_0, x_0, T_0, is not essential; however, it considerably facilitates the analysis of the possibilities of ion heating.

The results obtained are valid for plasma which is freely expanding into a medium without counterpressure and containing a fixed number of particles. In the case of a thick target (target dimensions much more than x_0), this corresponds to conditions under which it is possible to disregard the energy losses to electron

thermal conductivity. Below we discuss the possible role of thermal conductivity and also the pressure of powerful laser emission of ultrashort duration; calculations are made of the energy and duration of the emission pulse from the plasma.

II. Experimental Results

1. Heating Pulse

As a source of ultrashort pulses we used a laser on neodymium glass operating in the soft-synchronization mode; the emission wavelength was 1.06 μm. The laser characteristics are described in detail in [2].

The repetition intervals of ultrashort pulses, determined by the distance between the generator mirrors, was 15 ns. One pulse was separated from a pulse sequence by a special shutter with a 15 ns opening time. This pulse was then amplified.

As a result of examination, it was found that an individual pulse, as a rule, consisted of several peaks (subpulses) of different intensities, divided by different time intervals. Furthermore, it was explained, in accordance with the data from reference [6], that the generation time structure was not reproduced from burst to burst. Total duration of the laser pulse was approximately 10 ns. In this case, it contained several peaks with the average interval between them 1-2 ns. This time was determined by the relative position of the laser components. Total energy of the laser pulse was ∿0.1 J and usually was greater, the larger the peaks in the pulse. The duration of an individual peak can be assumed to fall within the interval from $2 \cdot 10^{-12}$ to $2 \cdot 10^{-11}$ s. The lower limit was obtained from measurements by the two-photon luminescence method, and the upper limit from measurements by an image converter and represents the time resolution of the image converter tube. It should be noted that in a number of experiments we intentionally attempted to increase the number of peaks in a laser pulse so as to more completely reveal the irregularities in the formation and heating of plasma under the effect of ultrashort pulses on a solid target.

4

2. Shadow Photography of Plasma with Illumination by Ultrashort Pulses

Methods of shadow photography with illumination by laser pulses of ns duration have been developed rather thoroughly [7]. In our experiments such methods were used as they applied to ultrashort pulses. The first measurement results were reported in [5]. The installation diagram is given in Fig. 1. The output emission of the laser passed through a KDP crystal and a small part of the light was transformed into a quadratic component (wavelength 0.53 μm). With the aid of a glass plate and a system of mirrors the area near the surface of the target was translucent with green light. In the focus of the lens with f = 200 mm was installed a blade which cut off part of the focal point. The edge of the blade in most of the experiments was directed perpendicularly to the surface of the target. In tnis case, after the laser burst a Schlieren photograph of the plasma was obtained, on which areas were reproduced with the refraction gradients along the surface of the target. In a number of experiments the blade was removed and shadow photographs of plasma were obtained. The image was recorded after a system of filters which separated the spectral region near 0.53 μm. Such filtration was used to reduce the effect of the natural emission of plasma.
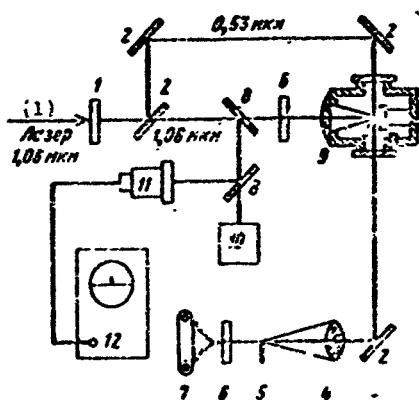

Fig. 1. Experiments in the shadow photography of plasma with the aid of ultrashort laser pulses: 1 — KDP crystals, 2 — mirror, 3 — target, 4 — lens, 5 — blade, 6 — filters, 7 — camera, 8 — glass plates, 9 — evacuated vessel, 10 — calorimeter, 11 — photocell, 12 — oscillograph.

KEY: (1) Laser. [мкм = μm].

Focusing of the heating emission was accomplished by a len, with f = 60 mm. The shape of the burst was recorded by a photocell wit. an oscillograph with the total resolution time approximately 1 ns. Because of delay, the sounding pulse came to the target 1.5 ns after the heating pulse.

Figure 2a depicts a shadow photograph of plasma at a chamber pressure of 10^{-2} torr. We obtained the image of a zone opaque for light with wavelength $\lambda = 0.53$ μm. After 1.5 ns the edge of the zone went away from the target a distance of $1.5 \cdot 10^{-2}$ cm, which corresponds to a rate of dispersion perpendicular to the surface of the target of $1 \cdot 10^7$ cm/s. Due to the dispersion of laser light on the heterogeneities of neodymium glass, the light beam of the quadratic component was inhomogeneous in cross section. In the photograph this is revealed in the nonuniformity of the background.

Graphic Not Reproducible
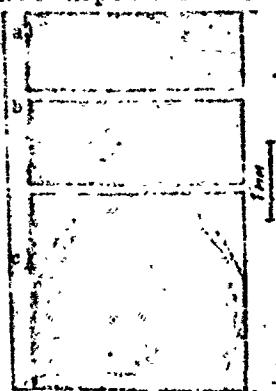
Fig. 2. Photograph of plasmas formed by ultrashort laser pulses: a) plasma expanding into vacuum; 1.5 ns after the arrival of laser pulse on target, shadow photography; b) the same, Schlieren photography; c) plasma expanding into air at a pressure of 7 torr, Schlieren photograph; the pressure shock front is seen 48 ns after the moment of formation.

The image in Fig. 2b is the Schlieren photograph of plasma with the same pressure in the chamber. The rate of dispersion of the area with large gradients of the refractive index in the direction away from the target, averaged for the first 1.5 ns after the effect of the pulse, is $(1-2) \cdot 10^7$ cm/s

Figure 2c is a Schlieren photograph of the process in air at a pressure of 7 torr. In this burst the target was acted upon by two pulses, ~6 ns apart. The front of the shock wave induced by the plasma and formed by the first pulse is noticeable. In the period 47.5 ns the wavefront moved away from the surface a distance of 2.3 mm; thus, the average speed is $5 \cdot 10^6$ cm/s. The velocity of the pressure shock front in a direction parallel to the surface of the target is $3 \cdot 10^6$ cm/s.

6

The presence of a time structure affects the results of the methods used differently. With shadow photography the opaque range of plasma, formed by any one subpulse, is recorded. On the Schlieren photograph of plasma the total effect of all subpulses is observed and the image can consist of a series of stripes. In the latter case, the processing of large numbers of photographs makes it possible to state that a velocity of 10^7 cm/s is characteristic for the conditions of our experiments.

3. The Photoregistration of Plasma Dispersion with the Aid of an Image Converter

Shadow procedures give the image of plasma at a fixed time. The continuous observation of the plasma process is possible when using the slotted scan method on an image converter tube. However, in this case, instead of two-dimensional registration, we obtain one-dimensional. Therefore, the shadow and image converter methods supplement each other.

The installation diagram is given in Fig. 3. The part of the laser pulse diverted from the beam by the glass plate was directed to the photocell starting the image converter tube. The remaining emission passed through the light delay system (corresponding to image converter starting delay) built on full internal reflection prisms and was focused on the target. Pressure in the chamber where the target was located could be varied from $5 \cdot 10^{-3}$ to $5 \cdot 10^{-6}$ torr. A plasma image in the necessary spectral range was built up on the image converter entrance slits with the aid of a lens. In a series of tests, along with plasma illumination laser pulse scanning was performed. In this case, the pulse was directed to the image converter tube with the aid of a glass plate and mirror through the filter.

The scanning rate of the image converter tube could be changed in stages from 10^7 to $1.5 \cdot 10^9$ cm/s [Translator's Note. The value of this exponent is not certain as this figure is extremely blurred in the original document.]. The instrument had a light amplification of $(2-3) \cdot 10^3$. Time resolution could reach $2 \cdot 10^{-11}$ s [8].
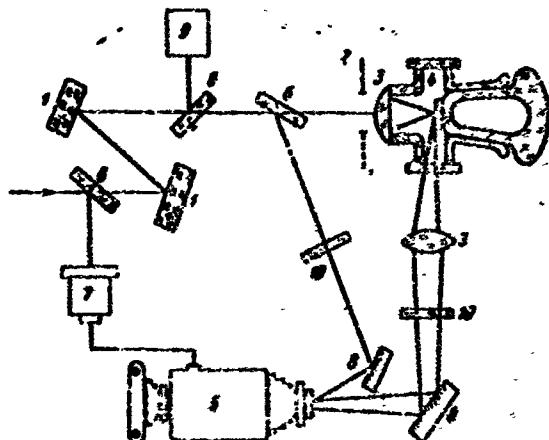
Fig. 3. The photoregistration of divergence with an image converter tube: 1 — internal reflection; 2 — diaphragm; 3 — lens; 4 — target; 5 — photoregistration image converter tubes; 6 — glass plates; 7 — photocells; 8 — mirror; 9 — calorimeter; 10 — filters.

Figure 4a gives the photograph of the scan of plasma radiation in the blue-green range of the spectrum (filter SZS-22). The entrance slits of the image converter tube were oriented perpendicularly to the surface of the target. A series effect of 3 pulses with an interval of 4 ns is noticeable. By the angle formed by the boundary of the area of noticeable brightness and by the direction of the axis of the time profile we can determine velocity. From the third pulse velocity is $(1.2 \pm 0.2) \cdot 10^7$ cm/s. The propagation velocity of brightness toward the laser varies from $0.8 \cdot 10^7$ to $1.5 \cdot 10^7$ cm/s from test to test. During dispersion, powerful plasma radiation is maintained in a small area which moves from the target with the velocity $\lesssim 3 \cdot 10^6$ cm/s. This area extends 0.2 mm from the target, which approximately coincides with the spatial resolution of the camera.

Graphic Not Reproducible
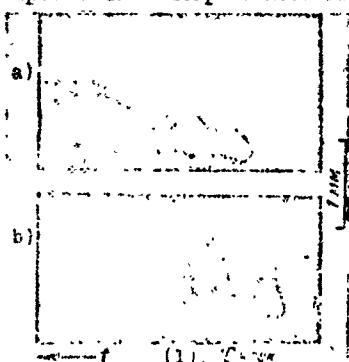
Fig. 4. Tracings of plasma dispersions on the image converter tube (target acted upon by several ultrashort laser pulses): a) plasma radiation scan; b) photoscan of plasma dispersion in scattered laser light (scattering angle ≈90°).

KEY: (1) ns.

8

Figure 4b is a photograph of laser light scattered on a target, obtained with an interference filter 100 $\overset{o}{A}$ wide. It is evident that intense dispersion at a 90° angle occurs in an area ~0.2 m. in length. This area coincides with the area of intense brightness (Fig. 4a) and moves with the same velocity ($3 \cdot 10^6$ cm/s). The weak vertical stripe in Fig. 4b has been caused by the dispersion of laser emissions from the plasma. With the sensitivity of the image converter tube to ultrashort pulses experimentally established, it was possible to evaluate the energy of diffuse elimination. It was equal (assuming isotropy) to a value comparable with total pulse energy.

Analysis of results shows that the heating and dispersion of plasma, which are observed on the image converter tube, can be presented according to the diagram in Fig. 5. In general, three stages of the process are observed. The first stage lasts 3 ns. In this stage, plasma is expanded with relatively low velocity ($3 \cdot 10^6$ cm/s) and laser emission strongly disperses. Both the first and subsequent pulses falling on the target during this time have no noticeable increase in velocity of dispersion.[1]
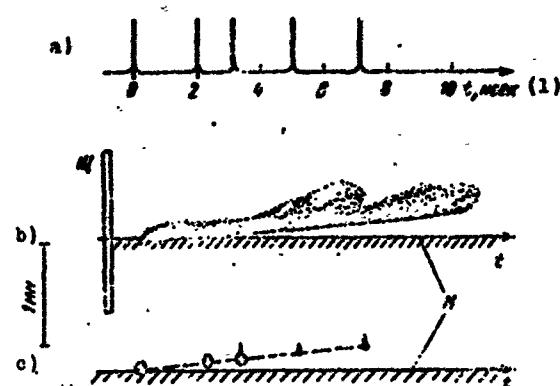

Fig. 5. Plasma dispersion during registration with image converter tube. a) time dependence of laser pulses; b) scan of plasma self-luminescence; c) time dependence of laser emissions scattered at an angle of 90°; Щ — slit position; M — boundary of target.

KEY: (1) ns.

If the pulse comes 3 ns later, it has a strong increase in velocity (10^7 cm/s). The second stage of the process is beginning.

---

[1]In this case, by pulses we mean subpulses (peaks) of the total laser pulse.

9

Pulses which arrive during this stage with a duration of 4 ns are dispersed more weakly than the previous ones. They give an additional rise in dispersion velocity; however, the numerical value of this increase is difficult to determine from photographs.

Finally, if an additional pulse arrives 7 ns after the initial moment, it marks the beginning of a new "triangular" dispersion. If pulses continue to arrive on the target, the picture observed on the image converter repeats with a period of 4 ns. Throughout the process (10-20 ns) the area of powerful dispersion which coincides with the zone of intense brightness moves away from the target at a velocity of less than $\leq 3 \cdot 10^6$ cm/s. Between this area and the target surface weak brightness is observed (Fig. 5b).

4. A Study of the Time Dependence of Laser Pulse Reflection

The emergence of a powerful reflection of laser emission when focusing ultrashort pulses on a target has already been noted [1, 2]. Total energy in the reflected light can reach 30% [2] and, consequently, is essential in the energy balance of plasma heating. A study of reflection is important not only from the point of view of decreasing this detrimental effect and increasing the efficiency of heating, but can also throw light on the processes which occur in plasma.

The time dependence of reflection was determined with the same image converter tube used in the above studies. The installation diagram is given in Fig. 6. Part of the laser emission was deflected by the glass plate to the photocell starting the image converter tube. After a light delay of 15 .. the basic emission was focused on the target in a vacuum of 10* torr [Translator's Note. The exponent * here is illegible in the original document.]. Direct and reflected emission was collected with the aid of lenses on small reflectors coated with magnesium oxide. The light scattered on the reflectors was directed to different parts of the input slot of the image converter tube. The optical paths of rays, in this case, were thoroughly shielded from each other. Registration was carried out at image converter scans of 80.20 and 3.5 ns.

10
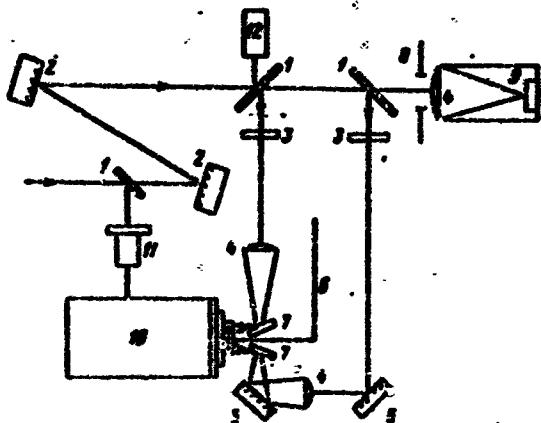
Fig. 6. Experiment on time dependence of reflected laser pulses: 1 — glass plates; 2 — total reflecting prisms; 3 — filters; 4 — lens; 5 — mirrors; 6 — light proof screen; 7 — magnesium oxide reflectors; 8 — diaphragms; 9 — target; 10 — moving-image camera with image converter tube; 11 — photocells; 12 — calorimeter.

In preliminary experiments it was established that reflection from plasma exceeds parasitic dispersion (reflection from the lens and the window of the evacuated vessel) by approximately 2-3 orders. The simultaneous scan of incident and reflected laser emissions is shown in Fig. 7. The first two pulses (peaks) 0.3 ns apart (Fig. 7b), are reflected more intensely than subsequent ones. The degree of reflection noticeably varies between 1 and 3 ns from the beginning of peaks (between the first and second groups). We can also note that within the weaker reflection stage a direct relationship is not observed between the intensity of reflected light and the intensity of incident light. Some pulses are reflected more weakly and others more powerfully. Sometimes present in reflected emissions are pulses which are so weak in the incident radiation that they do not appear on the photographic film. In Fig. 7a the number of pulses in the incident radiation is less than it is in Fig. 7b. The character of the reflection is the same; the first pulse is reflected more powerfully than subsequent ones. In this case, it is possible to determine that the degree of reflection varies noticeably during the time of the first pulse, which does not exceed 4 ns.

Sometimes in incident radiation the first peaks have so little of the total laser pulse energy that they are not visible on photographic film. According to estimations, their energy does not exceed 10^{-3} J. Such peaks are recorded in the channel for reflected emission because the sensitivity of this channel is higher. In this case, the reflection of the first incident pulse being recorded on the

11

film usually decreases. With powerful defocusing (an increase in the dimensions of the focal point to 1 mm) the degree of reflection was not changed noticeably during 10-20 ns.
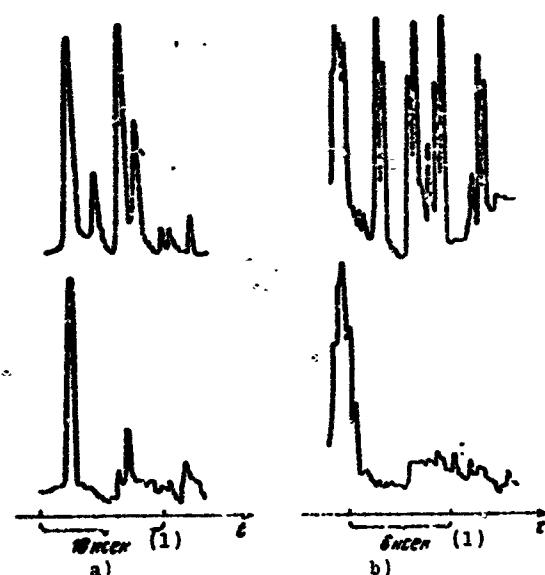

Fig. 7. Traces of laser emission (two cases): upper path — the incident laser pulse; lower path — the reflected.

KEY: (1) ns.

It is interesting to note that when focusing into air at atmospheric pressure, reflections from a spark could not be registered, which, apparently, is connected with the low density of the plasma formed. Therefore, it was possible to use a sample in air in our experiments in order to check the correctness of camera operation and the absence of parasitic reflexes.

5. X-ray Measurements of the
Electron Temperature of Plasma

The rate of dispersion, whose measurement was the basic purpose of the procedures discussed in Section II, §§ 2 and 3, is finally determined by the initial plasma temperature. The direct determination of electron temperature T_e was carried out by measuring the ratio of the X-ray continuum intensity into adjacent spectral regions separated by thin foil (see, for example, [9]). In that part of the spectrum where the emission is bremsstrahlung, the transmission of thin foil and thin films of various materials can be calculated [10]. This

12

method has even been used when the recombination continuum predominates
in the radiation since the dependence of intensity I on frequency ν
in both cases has the same form: $I\Delta v \sim \exp(-hv/kT_e)\Delta v$. The necessary
conditions for measurement correctness is the absence of line emission
in the investigated spectral ranges. In our case this was ensured
by checking the chemical analysis of the target. Line emission does
not fall in the pass band of beryllium filters used in the experiments
if the atomic number of the admixture is $Z < 9$. The portion of admix-
tures with $Z > 8$ in the lithium deuteride we used was a quantity <0.1%.

The diagram of the experiment is presented in Fig. 8. A lens
with $f = 60$ mm focused laser emission on the target which was located
in a vacuum of 10^{-3} torr. The X-ray radiation through beryllium windows
15 mm in diameter with the aid of plastic scintillators was recorded
by photomultipliers. The scintillators were made from polystyrene
with p-terphenyl and POPOP added; de-excitation time was ~2 ns. The
ЁLU-FT photomultipliers had gain factors of 10^6 and 10^8; their time
resolution was 5 ns. Signals from the photomultipliers were fed to
the input of a wide-band dual-trace oscillograph. On another oscillo-
graph with the aid of a photocell the laser pulse was monitored with
a time resolution of 1 ns.
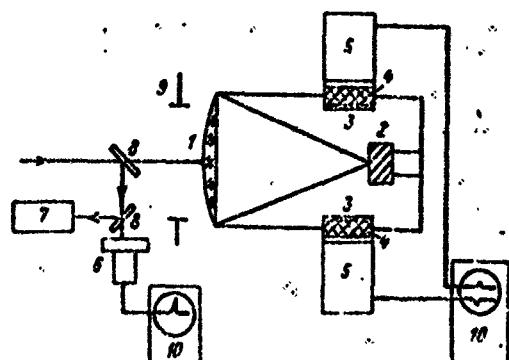
Fig. 8. Measurement of electron
temperature of plasma with respect to
X-ray emission: 1 — lens; 2 — tar-
get; 3 — beryllium filter; 4 —
scintillator; 5 — photomultiplier;
6 — photocell; 7 — calorimeter; 8 —
glass plates; 9 — diaphragm; 10 —
oscillograph.

Before measurements it was established that the contribution to
the signal of hard X-ray radiation as a result of the bremsstrahlung
of rapid electrons on the chamber walls [2] could be disregarded. For
this the direct X-ray radiation of plasma from the target, in one
registration channel, was shielded by polyethylene 0.8 mm thick. On

13

another channel, where changes were not made, the experimental conditions were controlled. Such a scheme served to check protection of the computers from the visible radiation of the plasma since polyethylene is transparent for the visible spectrum. As a result, it was found that the emission from the walls did not exceed the threshold of camera sensitivity.

The relative sensitivity of channels was determined from a comparison of signals obtained when using a filter of the same thickness (15 mg/cm^2). During measurements the filter thickness in one of the channels was doubled. Plasma temperature was determined with calculations performed in [10].

Experiments showed that the pulse duration of X-ray radiation was 5 ns, i.e., it was determined by time resolution. For laser pulse energy of 0.1-0.3 J, T_e, determined on the assumption of Maxwellian form of electron distribution function, varied from 140 to 220 eV for a main value of 180 eV. This corresponds to filter pass band from 4.5 to 10 $\overset{o}{A}$. In the channel where a fine filter was used and a photomultiplier with a gain factor of 10^6, the mean value of anode current was 1 A. For instance, for a specific burst with pulse energy 0.2 J the average anode current of the photomultiplier was 0.45 A and the temperature $T_e = 180$ eV.

The solid angle at which the scintillator was observed from the plasma region was 0.2 sr. The transmission of the beryllium filter 15 mg/cm^2 was $5 \cdot 10^{-5}$ [11]. After producing a rough evaluation of the conversion effectiveness of the scintillator and photoelectric cathode (number of photoelectrons per 1 keV of X-ray photons in the pass band of the filter) according to [12], we obtain radiant energy passing through the filter to the scintillator on the order of 10^{-2} erg and, consequently, the total energy of bremsstrahlung radiated by plasma in different directions is on the order of 10^4 erg. This estimate lays no claim to accuracy. However, it will be of use when evaluating $n_0 x_0$ (see Section III, paragraph 1) because of the low dependence of radiant energy upon plasma concentration.

III. Discussion of Experimental Results

1. Let us make a short review of the basic laboratory findings after emphasizing that the obtained results relate to laser pulses which consist not of one but of several peaks (subpulses). Experiments show that interaction of every subpulse with a target is not the same but depends upon the previous history and time of the peak sequence relative to the beginning of the process. At the initial moment we should assume the arrival of the first pulse (peak) at the target.

From the results obtained it follows that the first pulses (following in 3 ns) form the plasma which moved away at a low $(3 \cdot 10^6$ cm/s) velocity (see Section II, § 3, and Fig. 5). At approximately the same time we observe the intense reflection of laser emission at an angle of 180° and lateral dispersion (the reflection) at an angle of 90° to the direction of the incident beam. A small fraction of the total energy is spent on the formation of the initial plasma. This is apparent from the fact that the first pulses with initial energy 10^{-2}-10^{-3} J are recorded on the photographic film in the emission reflected at an angle of 180°. For comparison let us say that in order to ionize and heat, to a temperature of several electron volts, a layer of the target with an area equal to the area of the focusing spot $(3 \cdot 10^{-4}$ cm^2) and a thickness x_0 equal to the wavelength of laser emission ($\sim$1 μm), it is necessary to expend energy on the order of 10^{-3} J.

After 3 ns the possibility arises of further heating the plasma This is indicated by the high dispersion rate of the plasma (up to $1.5 \cdot 10^7$ cm/s) observed during the registration of plasma brightness on the image converter tube as well as in shadow photographs. Furthermore, a noticeable decrease in intensity of laser emission reflected at angles of 180 and 90° is noticed. In 4 ns the pulses arriving at the target are absorbed by the hot plasma which has been formed, as is apparent in Fig. 4. After 7 ns (if the next pulse arrives) on the image converter tube we observe the formation of a new portion of high-temperature plasma which moves away at a velocity of $1 \cdot 10^7$ cm/s.

15

If pulses continue to enter the target, the pattern is repeated with a period of 4 ns.

During the entire process, a layer of slowly $(3 \cdot 10^6$ cm/s) dispersing plasma is observed near the target. This is indicated by photographs of both the plasma radiation scan and the lateral dispersion (reflection) scan.

The X-ray measurements of the electron temperature of the plasma give a mean value of 180 eV. Under such conditions electron-ion relaxations will be able to occur for substantial gas-dynamic expansion (see section V) and, therefore, a recalculation of the initial electron temperature (right after the arrival of the pulse which gives the high-temperature heating) leads to a value of $T_0 = 270$ eV. Determining the electron temperature from the dispersion rate observed from the image converter tube and shadow photographs gives a value of $T_0 \simeq 70\text{-}160$ eV [see formula (16)]. As has already been mentioned, these measurements were made on different laser bursts; therefore, it is natural to assume that the difference obtained was caused by the difference in the parameters of laser emission.

The longitudinal dimension x_0 of hot plasma at the initial moment can be determined from the dispersion of the glowing region in its own and the reflected light of the laser, scattered at an angle of ~90° to the incident beam. The value of $x_0 \leq 9 \cdot 10^{-2}$ cm. On the other hand, from the shadow and Schlieren photographs, which give an idea of the dimensions of the region occupied by rather dense plasma $n_e \approx 10^{21}$ cm^{-3}, we obtained $x_0 \simeq (1\text{-}2) \cdot 10^{-2}$ cm. The same values are obtained if we take into account the total energy of X-ray radiation (see Section II, § 5). This energy is proportional to the product of $n_0 V_0$, where V_0 is the initial volume of hot plasma. Since the radius of the focal point is known we obtain, with the aid of the formulas below (20), (28), an estimated value of $n_0 x_0 \simeq 10^{19}$ cm^{-2} which, when $x_0 \simeq 10^{-2}$ cm, corresponds to $n_0 \simeq 10^{21}$ cm^{-3}. A layer of the solid target with a thickness approximately equal to the wavelength of the laser emission becomes hot plasma.

16

2. On the basis of the experimental data discussed, the following model of the formation and dispersion of the plasma under the effect of several ultrashort intense laser pulses on a target is the most probable model. A small part of the energy in the first pulse goes to the single initial ionization of the lithium deuteride layer with a thickness of an order equal to the wavelength of laser emission. Simultaneously with the ionization there occurs a heating of the formed plasma to a temperature of several electron volts. Further temperature rise is halted due to the fact that plasma frequency $\omega_p \sim \left(\frac{4\pi n e^2}{m_e}\right)^{1/2}$ [13] rapidly becomes greater than the frequency ω of the laser light. Because of this, the remaining part of the pulse is effectively reflected.

The initial plasma formed moves away relatively slowly. Subsequent ultrashort pulses continue to be strongly reflected until particle density due to expansion falls to a magnitude determined by the condition

$$\left(\frac{4\pi Z n e^2}{m}\right)^{1/2} < \omega, \tag{1}$$

where Z is the average number of electrons, taking into account one atom of the parent substance of the target, and n is the total density of atoms and ions.

At the moment when plasma density falls to the values determined by (1), laser pulses begin to be effectively absorbed, forming high-temperature plasma which moves away with high velocity. The portion of reflected light noticeably decreases. For a certain period of time, the hot plasma formed is nontransparent for laser emission. After transparency sets in, the next laser pulse penetrates again to the target and forms a new portion of high-temperature plasma.

The observed reflection of the first pulses at an angle of 180° and dispersion at an angle of 90° to incident emission are apparently part of one and the same process, the reflection which appears upon the breakdown of condition (1). The experimental data show that the

17

character of reflection for targets of lithium deuteride (obtained by compression) does not differ greatly from isotropic; however, the first pulse is reflected in a smaller solid angle.

From the data it follows that upon focusing ultrashort pulses with energy of 0.1 J, a noticeable variation is not observed in the condition of the reflection of light from plasma when $\omega_p > \omega$.

IV. Emission and Thermal Conductivity of Plasma. An Evaluation of the Effect of Laser Emission Pressure

1. Thermal conductivity, leading to an additional increase in the number of heated particles, can play a substantial role in the high-temperature heating of plasma by laser pulses. In our case, we can disregard radiant thermal conductivity since plasma is optically fine, and assume that the basic mechanism for the heat transfer is electronic thermal conductivity. We shall also assume that the initial heating of electrons from temperature T_0 occurs in a finite domain with dimension x_0 and then this region is expanded because of thermal conductivity. Near the front of a thermal wave, as is known (see, for example, [14])

$$T_e(x,t) = T_e(t) \left[1 - \frac{x}{x_\phi} \right]^{2/3}, \tag{2}$$

where x_ϕ is the coordinate of the front of the thermal wave.

Let us substitute $T_e(x, t)$ into the heat equation:

$$\frac{5}{2} n_e \frac{\partial T_e}{\partial t} = a \frac{\partial}{\partial x} T_e^{5/2} \frac{\partial T_e}{\partial x}, \tag{3}$$

where $a \approx 10^{50}$ CGS units; T_e is in ergs.

Passing to the limit $x \to x_\phi$ and integrating the obtained expression, while taking into account the law of conservation of energy, under boundary conditions $t = 0$, $x_\phi = x_0$, we find

18

$$x_0 = [6.1 \cdot 10^{10} (Q/S)^{5/3} n_e^{-7/3} t + x_0^{3/2}]^{2/3},$$ (4)

where Q is the plasma energy in erg when t = 0; S is the area of the focusing spot of the laser emission on the surface of the target in cm^2.

Maximum propagation velocity for the thermal wave is

$$\frac{dx_0}{dt}\Big|_{t=0} = 1.35 \cdot 10^{10} \left(\frac{Q}{S}\right)^{5/2} (n_e x_e)^{-7/2}.$$ (5)

Equating this velocity with the asymptotic velocity of plasma dispersion $v_m = (3ZT_e/m_i)^{1/2}$, we obtain the relationship, which is virtually independent of the form of ions,

$$T_0^{xp} = 1.5 \cdot 10^{-10} (n_e x_e)^{1/2} \text{ keV}.$$ (6)

Thermal conductivity during dispersion and relaxation of plasma can be disregarded if $T_e < T_0^{xp}$. If $|T_e \geq T_0^{xp}|$, it is necessary to take thermal conducitvity into account. At $n_0 x_0 \approx 10^{19}$ cm^{-2} temperature $T_0^{xp} \approx 500$ eV; therefore, for our case, we may disregard thermal conductivity.

2. Let us examine the regularities of plasma emission during dispersion. For lithium deuteride, plasma emission, beginning with ~100 eV, is basically bremsstrahlung (see, for example, [14]). At lower temperature, recombination emission predominates.

The need to examine the emission process is connected with the following facts. In the first place, the essence of one of the experimental methods — the X-ray method — lies in the measurement of radiant energy in certain sections of the spectrum (see Section II, § 5). In this case, integration in time occurs because the emission pulse duration is shorter than the time which can be resolved by the metering arrangement. In the second place, it will be necessary to account for emission in the calculations of electron-ion relaxation (see Section V).

19

The intensity of the bremsstrahlung, which we shall examine subsequently, is described by the following expression [19]:

$$I_{\gamma} = 1.34 \cdot 10^{-11} Z^2 n_e n_i T_e^{1/2} \quad \text{erg/cm}^3 \cdot \text{s}. \tag{7}$$

Emission can be considered three-dimensional if the mean free path l_{γ} of the braking quanta in the plasma [14]

$$l_{\gamma} = 1.53 \cdot 10^{39} \frac{T_e^{7/2}}{Z^2 n_e n_i} \quad cm.$$

(where T_e is expressed in degrees Kelvin) is a much more characteristic dimension of plasma x_0. We will consider this condition to be fulfilled. For instance, for lithium deuteride at $T_e = 200$ eV, $n_e = 10^{21}$ cm^{-3}, calculation shows that $l_{\gamma} \approx 3.6 \cdot 10^2$ $cm \gg x_0 \approx 10^{-2}$ cm. We will also examine temperature $T_e \gtrsim 100$ eV and assume the plasma to be fully ionized.

In pulse action time $\tau = 10^{-11} - 10^{-12}$ s, electrons heated to a temperature of $T_e \gtrsim 100$ eV cannot transmit any substantial portion of their energy to ions. Equalization time for electron and ion temperatures is [13]

$$\tau_{ei} = \frac{3}{8\sqrt{2\pi}} \frac{m_i T_e^{3/2}}{m_e^{1/2} e^4 n_i Z^2 \ln \Lambda}, \tag{8}$$

where $\ln \Lambda \approx 5$ is the Coulomb logarithm. For lithium deuteride at $n_e = 5 \cdot 10^{20}$ cm^{-3} and $T_e = 200$ eV, this time $\tau_{ei} \approx 3 \cdot 10^{-10}$ s. Consequently, condition

$$\tau_{ei} \gg \tau \tag{9}$$

is fulfilled throughout the range of temperatures in question.

Thus, initially, we have plasma occupying volume V_0 with electron concentration n_0 and electron temperature T_0. Considering (9), we obtain $T_i|_{t=0} = 0$

20

Plasma at the moment of formation, as well as during dispersion, is not uniform. Its temperature and density are characterized by a certain spatial distribution. We do not consider this distribution and we examine the values of the parameters averaged throughout the volume. On the one hand, this is done because the initial density and temperature profiles are known; on the other hand, the majority of experimental procedures (including those described above) give plasma characteristics averaged by volume.

Let us first examine two-dimensional plasma dispersion, i.e., when the thickness of the plasma layer $x \ll d$, where d is the diameter of the focusing spot. Let us take the following designations: $n = Zn_i$ (Z is the average ion charge), M is the average mass of ions. For lithium deuteride $Z \approx 2$, $M \approx 4m_H$, where m_H is the atomic mass of hydrogen. From the equation of motion for the plasma volume as a whole

$$PdV = dE_{кин},$$ (10)

where $P = n\left(T_e + \frac{1}{2}T_i\right)$ — the pressure of plasma; $n = n_* x_*/x$; $V = Sx$: S is the area of the heated surface; $E_{кин}$ is the energy of the directed motion of ions (contribution of electrons $\sim m_e/M$); after substitution, we obtain the equation of motion in the calculation for one ion:

$$ZT_e + T_i = M\dot{x}\ddot{x}.$$ (11)

Here and subsequently the CGS system of units is used; T — in ergs (with the exception of specifically stipulated cases), $\dot{x}$, $\ddot{x}$ are the time derivatives.

The law of conservation of energy is written in the form

$$-\frac{3}{2}\frac{d}{dt}(ZT_e + T_i) = \frac{M}{2}\frac{d}{dt}\dot{x}^2 + i(t).$$ (12)

where i(t) is emission intensity in the calculation of one ion. Taking into account (7), expression (12) assumes the following form:

21

$$\frac{d}{dt}(ZT_e + T_i) = -\frac{M}{3}\frac{d}{dt}\dot{x}^2 - 0.9 \cdot 10^{-19} Z^2 n_0 x_0 \frac{T_e^{1/2}}{x}. \tag{13}$$

The solution of equations (11)-(13) gives the following results. If we designate by Q_0 the energy released in plasma at moment t = 0 and by $E_{\text{гд}}$ the kinetic energy of directed motion of ions with $t \to \infty$, then $E_{\text{гд}}/Q_0 = f(T_0/n_0 x_0)$ at the given values of Z and M, when

$E_{\text{изл}}/Q_0 = 1 - (E_{\text{гд}}/Q_0)$. In Fig. 9 the solid curve illustrates this dependence for lithium deuteride in the case of two-dimensional dispersion. For other values of Z and M, scale $T_0/n_0 x_0$ is multiplied by $(Z^2/10)(M/m_H)^{1/2}$. The approximate solution of the spherical case is carried out similarly.
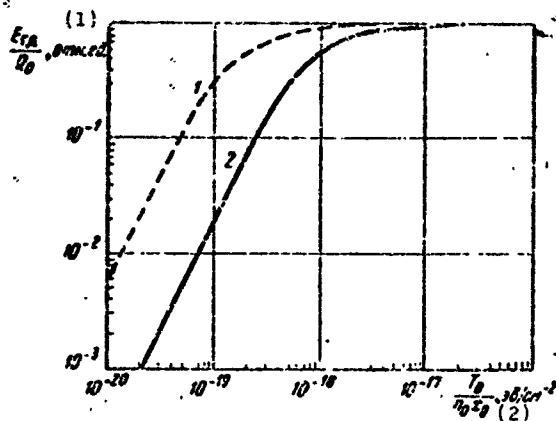
Fig. 9. The dependence of the ratio of the energy of the asymptotic motion of plasma $E_{\text{гд}}$ to the total energy of the laser pulse Q_0 applied to the plasma on the initial parameters of the limited (without thermal conductivity) plasma: temperature T_0, density n_0 and thickness x_0 (radius r_0). 1 — spherical dispersion; 2 — two-dimensional dispersion.
KEY: (1) rel. unit; (2) eV/cm^{-2}.

For lithium deuteride at $n_0 x_0 = 10^{19}$ cm^{-2} and $T_0 = 200$ eV the losses to radiation are small, which is also confirmed by experiment (see Section II, § 5). For the prescribed value of S, the total number of heated particles $N \approx n_0 x_0$; therefore, as can be seen from Fig. 9, the role of emission increases with an increase in N when T_0 is constant, and when N = const it decreases with an increase in T_0.

Without allowing for emission for flat and spherical dispersion, it is possible to obtain the following expressions:

$$\dot{x} = \left[\frac{3ZT_e}{M}\left(1 - \left(\frac{x_0}{x}\right)^{2/3}\right)\right]^{1/2}, \tag{14}$$

$$T_e + \frac{1}{Z}T_i = T_0\left(\frac{x_0}{x}\right)^{2/3}, \tag{15}$$

22

$$\dot{r} = \left[\frac{\varkappa \varkappa T_0}{M}\left(1 - \frac{r_0^3}{r^3}\right)\right]^{1/2}.\qquad(16)$$

$$T_e + \frac{1}{Z}T_f = T_0\left(\frac{r_0}{r}\right)^3.\qquad(17)$$

Unlike two-dimensional dispersion, in spherical dispersion when
$r/r_0 = 3\text{-}4$, plasma temperature falls by one order and dispersion rate
is close to asymptotic.

3. Let us examine the features of plasma emission. For this
we will return to the dependence graphically presented in Fig. 9. It
is possible to see that in the region where $E_\square \approx Q_0$, total radiant
energy is determined with great error. In this case, which occurs
in the experiment, emission and gas-dynamic dispersion are independent
processes. The bremsstrahlung energy from plasma takes the form

$$I(t) = a_0 \int_0^t n_e^2 T_e^{1/2} V \, dt.\qquad(18)$$

Assuming that electron and ion temperatures equalize before the
basic component of radiant energy is illuminated, with the aid of
(16) and (17) we have obtained the following expression for the time
dependence of bremsstrahlung:

$$I(t) = A\left(\frac{w}{1+w^2} + \operatorname{arctg} w\right),\qquad(19)$$

where A is a constant depending upon initial conditions; $w = \left(\frac{3ZT_0}{Ar_0^2}\right)^{1/2} t.$

It is assumed that plasma at the initial moment has a density of
$n_e = n_0$ and temperature $T_e = T_0$, while we examine dispersion of a
hemisphere with initial radius r_0, which is determined from condition
$S = \pi r_0^2$ where S is the area of the focusing spot.

The total energy radiated by plasma does not depend upon
temperature:

$$I_{\phi\phi}(\infty) = 4.0 \cdot 10^{-30} \frac{SZM^{1/2}(n_e r_0)^3}{\sqrt{1+Z}}\qquad(20)$$

23

For lithium deuteride with spherical dispersion and initial parameter determined from experiment ($n_0 r_0 = 10^{20}$ cm^{-2}), we obtain $I_{2n}(\infty) \cong 1.5 \cdot 1$ erg.

The decrease in emission $dI/dt \sim 1/(1+w^3)^2$ and, consequently, characteristic pulse time $\tau_{изл}$, can be evaluated from condition

$$w(\tau_{изл}) = 1. \qquad (21)$$

For time

$$\tau_{изл} = r_0 \sqrt{\frac{M}{32 T_0}} = \frac{r_0}{r_\infty} \qquad (22)$$

82% of the energy is radiated:

$$I(\tau_{изл}) = 0.82 I(\infty).$$

In the experiment (see II, § 5) X-ray radiation was measured with the use of filters with a pass band limited on the side of longer waves. For a beryllium filter 15 mg/cm^2 the boundary wavelength is 8 Å. The intensity of bremsstrahlung in the range of the X-ray continuum depends exponentially upon wavelength:

$$I_\lambda d\lambda \sim \exp(-hc_i/\lambda T)\, d\lambda.$$

In order to determine the energy passing through the filter, it is necessary to integrate the product of the filter transmission and spectrum: $I = \int_0^\infty I_\lambda B_\lambda d\lambda$, where B_λ is the spectral characteristic of filter transmission. However, for beryllium filters it is possible to assume with a sufficient degree of accuracy $I = \int_0^\lambda I_\lambda d\lambda$.

Thus, the energy passed through the filter is

$$I_{\lambda_0}(t) = \exp\left(-\frac{hc}{\lambda_0 T}\right) I(t). \qquad (23)$$

24

This energy decreases with time according to the following law:

$$\frac{dI_{\lambda_0}}{dt} \sim (1 + \alpha t)^{-3} \exp(-\alpha t), \tag{24}$$

where $a = \frac{hc}{\lambda_0 T_0}\left(1 + \frac{1}{Z}\right).$ When $\lambda_0 = 8$ Å and $T_0 = 200$ eV, $a = 11.4$.

The characteristic time of the emission which has passed through the filter $\tau_{max}^{\lambda_0}$ is determined from relationship

$$\omega \sqrt{a} = 1. \tag{25}$$

Thus, we obtain

$$\tau_{max}^{\lambda_0} = \frac{1}{\sqrt{a}}\,\tau_{max}. \tag{26}$$

Emission duration with variable focusing depends only upon initial temperature.

Integral values of $I_{\lambda_0}(\infty)$ and $I(\infty)$ are connected by the approximate relationship

$$I_{\lambda_0}(\infty) \approx a^{1/3}\, e^{-a}\, I(\infty). \tag{27}$$

For lithium deuteride, in our case, we have $I_{\lambda_0}(\infty) \approx 0.25$ erg, $\tau_{max} \approx 0.5$ ns, $\tau_{max}^{\lambda} \approx 0.2$ ns.

In the case of two-dimensional dispersion, total radiant energy is also independent of temperature:

$$I_{\mathit{ns}}(\infty) = 3.6 \cdot 10^{-19} \frac{\sqrt{Z} A^{1/2} (n_0 x_0)^2}{\sqrt{1+Z}}. \tag{28}$$

For lithium deuteride under these conditions, we obtain $I_{\mathit{rn}}(\infty) = 4 \cdot 10^1$ erg, i.e., one order of magnitude greater than with spherical dispersion. For two-dimensional dispersion the quantity $I_{\lambda_0}(\infty)$ is evaluated according to formula (27).

25

Since there is an intermediate case between two-dimensional and spherical dispersion in the experiment, the total radiated energy must fall between $I_{c\phi}(\infty)$ and $I_{n\eta}(\infty)$, i.e., for $n_0 r_0 = 10^{19}$ cm^{-2} between $4 \cdot 10^4$ and $4.5 \cdot 10^3$ erg. The evaluation obtained from experimental measurements gives

$$I(\infty) \approx 10^4 \ \text{erg}.$$

4. The possible effect of the pressure of laser emission on the plasma being formed deserves consideration. The observation of such an effect during the focusing of nanosecond laser pulses on a solid target was discussed in [15]. In the case we examined, the fluxes near the target are considerably higher and, consequently, greater than the value of light pressure.

The total pulse which can be transmitted from an electromagnetic wave to plasma is expressed in the following manner:

$$P_t \sim \frac{1}{s} W,\tag{29}$$

where W is the laser pulse energy.

On the other hand, taking into account the fact that the basic component of the emission goes into heating, we obtain

$$W \sim NT_e.\tag{30}$$

Here N is the number of ions participating in the heating and T_0 is initial temperature (in energy units).

The gas-dynamic pulse of plasma is expressed by

$$P_{r\mathbf{x}} \sim \frac{NT_s}{v_\infty},\tag{31}$$

where v_∞ is the asymptotic rate of dispersion. Taking into account (30) and (31), expression (29) assumes the form

26

$$P_e \sim \frac{v_{so}}{c} P_{or}$$ (32)

In the above described experiments $v_{so} \approx 10^7$ cm/s and $P_e \sim 10^{-3} P_{ra}$ and, consequently, the effect of the pressure of laser emission can be disregarded.

V. Electron-Ion Relaxation in Plasma Formed by a Powerful Ultra-short Laser Pulse

1. The problem of heating plasma is primarily the problem of achieving high ion temperature. During laser heating electrons are heated first, basically because of a process opposite to bremsstrahlung. Ions obtain heat from electrons as a result of collisions. At high initial electron temperatures, which can be attained by focusing of powerful ultrashort pulses, plasma can disperse before a temperature balance of its components occurs. The need for taking this non-equilibrium into account was considered in [5].

The heating of electrons occurs during a pulse duration of $\tau = 10^{-11}$-10^{-12} s. In most of the cases of practical interest this time is much less than the characteristic times of electron-ion relaxation τ_{ei} and gas-dynamic expansion τ_{-A}. For example, for plasma parameters in the described experiments $n_e \approx 10^{71}$ cm^{-3}, $T_e \approx 200$ eV and $x_0 \approx 10^{-3}$ cm, we obtain $\tau_{ei} \approx 10^{-10}$ s, $\tau_{rA} \approx 10^{-9}$ s. However, the electron-electron relaxation time $\tau_{oe} \approx 10^{-12}$ s. Therefore, below we will use the idea of instantaneous heating of electrons to temperature T_0. The temperature of ions at initial moment $T_1(0) \ll T_0$ and, without reducing accuracy, we set $T_1(0) = 0$. We will be concerned with temperatures of $T_e \lesssim 100$ eV at which plasma is completely ionized. At the initial moment electron density is n_0 and the plasma dimensions are known. At this time free dispersion of the plasma begins under the action of internal pressure and emission and electron-ion relaxation simultaneously. With the same considerations as presented in Section IV, paragraph 2 we will consider that during expansion, density and temperature are uniform in the entire plasma volume.

27

Since in our experiments the character of the dispersion changes in time ~τ_{rA} from two-dimensional to spherical, let us examine both these types. We emphasize once again that we are speaking of confined plasma. Such a condition in practice corresponds to the condition of heating thin foil or a small isolated particle. During the heating of a thick target (target volume much greater than initial volume of plasma) thermal conductivity can play a significant role (see Section IV, paragraph 1).

With an increase in initial electron temperature T_0 the relaxation rate falls and the expansion rate of the plasma increases. Temperature T^*_0, at which the characteristic dispersion time τ_{rA} is comparable with the equalization time of electron and ion temperature τ_{ei}, determines a certain critical value of initial thermal energy. At $T_0 < T^*_0$ the heating of ions can be considered effective. Relaxation manages to occur before a pronounced temperature drop due to the adiabatic expansion of plasma. At $T_0 > T^*_0$, on the other hand, dispersion proceeds faster than heat transfer from electrons to ions.

Let us evaluate T^*_0. Since

$$\tau_{ei} = \frac{3}{8\sqrt{2\pi}} = \frac{M T_e^{3/2}}{Z^2 e^4 n_e m_e^{1/2} \ln\Lambda} \qquad (33)$$

$$\tau_{rA} \sim \frac{x_0}{v_{3e}} = x_0 \left(\frac{5}{3} \frac{Z T_e}{M} \right)^{-1/2} \qquad (34)$$

(where v_{3e} is the speed of sound), then from condition $\tau_{ei}(T^*_e) = \tau_{rA}(T^*_e)$ we obtain

$$T^*_e = 1.4 \cdot 10^{-9} \frac{e^2 Z^{3/4} m_e^{1/4} (\ln\Lambda)^{1/2}}{M^{1.4}} (n_e x_e)^{1/2} \quad \text{eV}. \qquad (35)$$

For lithium deuteride at $n_0 x_0 = 10^{19}$ cm^{-2} (as in our experiments) we obtain $T^*_0 = 450$ eV. More precise calculations give a value of $T^*_0 = 600$ eV.

28

2. Let us examine a two-dimensional layer of plasma with initial thickness x_0. The rate of electron-ion relaxation in the absence of any energy losses can be written in the form [13]

$$\frac{dT_e}{dt} = -\frac{T_e - T_i}{\tau_{ei}} = -\frac{8\sqrt{\pi}}{3} \frac{e^2 Z^2 n_e^{1/2} m_e \ln \Lambda}{M T_e^{3/2}} (T_e - T_i).$$ (36)

From the table of values presented in [13] we shall select $\ln \Lambda = 5$. Expression (36) is valid with both small and large differences $T_e - T_i$ [16]. Substituting numerical values and replacing $n_i = n_0 x_0 / Zx$, we obtain

$$\frac{dT_e}{dt} = -\frac{\alpha x_0}{Zx} \frac{T_e - T_i}{T_e^{3/2}}.$$ (37)

where $x = 5.33 \cdot 10^{-19} (2 n_e / M)$.

Besides energy losses upon collision with colder ions, electrons lose thermal energy on their acceleration and also on emission. Ions acquire heat because of relaxation but they lose it only on gas-dynamic expansion. From the equation of motion for the plasma volume as a whole

$$(P_e + P_i) \frac{dV}{dt} = \frac{dE_{нин}}{dt}$$ (38)

(where P is pressure, V is volume, $E_{нин}$ is the energy of directed motion of plasma), we may conclude that the contribution of each of the components to the energy gain of dispersion is proportional to $ZT_e / (ZT_e + T_i)$ and $T_i / (ZT_e + T_i)$ for electrons and ions, respectively.

This conclusion is justified by the following facts. In the first place, we deal with colliding plasma, i.e., $l_e \ll x_0$. Here l_e is the length of the mean free path of electrons which, according to [17], can be evaluated by expression

$$l_e \sim v_e \tau_e \approx 6 \cdot 10^{11} \frac{T_e^2}{n_i},$$ (39)

29

where T_e is in keV. For example, for $n_i = 5 \cdot 10^{20}$ cm^{-3} and $T_e = 0.2$ keV we obtain $l_e = 5 \cdot 10^{-5}$ cm $\ll x_0 \simeq 10^{-2}$ cm.

In the second place, we can disregard the acceleration of ions by electrons at the edge of the freely expanding plasma. Plasma volume $V_y \sim S l_D$ will be captured by such acceleration. Here S is the focusing area and l_D is the Debye screening distance, equal to

$$ l_D = \left(\frac{kT_e}{4\pi n_e r^2} \right)^{1/2} \approx 2 \cdot 10^3 \left(\frac{T_e}{n_e} \right)^{1/2}, \tag{40} $$

where T_e is in eV.

Volume V_y composes a small portion of the total volume V of the plasma: $V_y \sim (l_D/x)V$. For example, for $n_e \approx 10^{21}$ cm^{-3}, $T_e = 1$ keV we obtain $l_D \approx 7 \times 10^{-7}$ cm and $V_y \approx 10^{-4} V$ when $x_0 = 10^{-2}$ cm.

Hence, we obtain the following equations of relaxation for electrons and ions:

$$ Z \frac{dT_e}{dt} = -\varkappa \frac{x_0}{x} \frac{T_e - T_i}{T_e^{3/2}} - \frac{2}{3} M \dot{x} \ddot{x} \frac{ZT_e}{ZT_e + T_i} - \frac{2}{3} i(t), \tag{41} $$

$$ \frac{dT_i}{dt} = \varkappa \frac{x_0}{x} \frac{T_e - T_i}{T_e^{3/2}} - \frac{2}{3} M \dot{x} \ddot{x} \frac{T_i}{ZT_e + T_i}. \tag{42} $$

where i is the intensity of radiation in the calculation for one ion.

The addition of (41) and (42) leads us, of course, to equation (12), which upon substitution of i(t) assumes the form (13). Equation (38) with the appropriate substitutions is reduced to (11).

Thus, the system of equations (11), (13), (42) determines the problem proposed. Its solution has been examined in reference [20].

3. The solution of the system of equations (11), (13), (42) is carried out by approximation but possible errors do not exceed 20%.

30

Results have been obtained in analytical form; however, the dependences found are complex and assigned parametrically. Therefore, we will not give them here, but for the cases interesting us let us present results on graphs.

The dependence of ion temperature on time $T_1(t)$ has a certain maximum T_{1m} when $t = \tau_m$, determined by the initial conditions of the problem. It is precisely this quantity which is of practical interest to us. Figure 10 gives dependence $T_{1m}(T_0)$ for lithium deuteride when $n_0 r_0 = n_0 x_0 = 10^{19}$ cm^{-2}. The change to plasma of another composition and initial data is accomplished by means of the multiplication of the scale along the axis of ordinates by the quantity

$$\left(\frac{3}{2}\,\frac{Z}{1+Z}\right)^{1/2}\left(\frac{8m_H}{M}\right)^{1/4}\frac{Z^{3/4}}{2.25}\sqrt{\frac{n_0 x_0}{(n_0 x_0)_{t=0}}}.$$

and of the scale along the axis of the abscissas by the quantity

$$\left(\frac{2}{3}\,\frac{1+Z}{Z}\right)^{1/2}\left(\frac{8m_H}{M}\right)^{1/4}\frac{Z^{3/4}}{2.25}\sqrt{\frac{n_0 x_0}{(n_0 x_0)_{t=0}}}.$$

Let us note that when selecting Z for plasma consisting of several elements, we should use a root-mean-square evaluation $Z = \tilde{Z} = \sqrt{\sum_i Z_i^2}$, with which the number of electrons for one ion $\tilde{Z}$ must be near Z. For M we can assume a mean arithmetic value. For lithium deuteride, for example, Z = 2.25; $\tilde{Z}$ = 2; $M = 4m_H$.
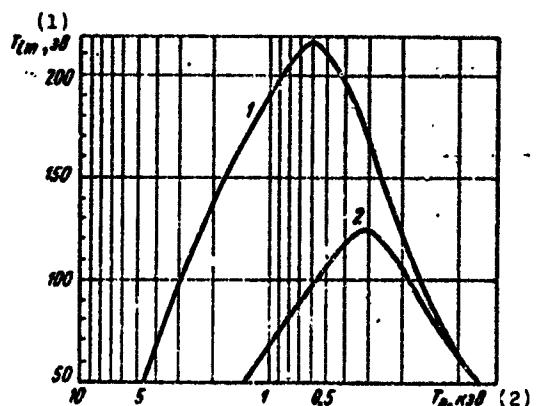
Fig. 10. Dependence of maximum ion temperature T_{1m} on initial electron temperature T_0 for confined plasma: 1 — two-dimensional dispersion; 2 — spherical dispersion.

KEY: (1) s; (2) keV.

31

Figure 11 presents with the solid lines the dependence $\tau_m(T_0)$ at given values of n_0, r_0, x_0. We should keep in mind that in the two-dimensional case, at sufficiently high T_0, the ratio $x_m/x_0 > 3$ and, therefore, dispersion acquires a spherical character. Figure 11 shows with the dotted line how the dependence of this case will actually be modified.
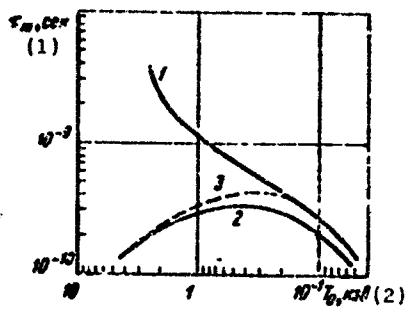
Fig. 11. Effective time τ_m of maximum ion temperature existence as a function of initial electron temperature for lithium deuteride when $n_0 = 10^{21}$ cm^{-3}, $x_0 = r_0 = 10^{-2}$ cm: 1 — two-dimensional dispersion; 2 — spherical dispersion; 3 — a change from two-dimensional dispersion to spherical under the conditions of the experiments conducted.

KEY: (1) s; (2) keV.

In the region of low T_0, the drop in τ_m is explained by the pronounced decrease of τ_{ei} as compared with $\tau_{гд}$ and $\tau_{изл}$ [see formulas (33), (34), (22)]. In this case, the temperature endurance will be determined by the latter, more gradual, process and, therefore, will increase.

4. The analysis of the solutions obtained shows that for limited (without thermal conductivity) plasma, the dependence of the highest attainable temperature for ions T_{im} on the initial electron temperature T_0 can be broken down into three regions. In the region of low T_0 where emission can be substantial, electron-ion relaxation occurs before gas-dynamic expansion has time to develop. Subsequently, ions and electrons began to disperse with identical temperatures. With an increase in T_0 a region begins where electron relaxation occurs during dispersion. The increase in T_{im} rapidly decelerates with an increase in T_0. Finally, at high T_0, plasma, under the action of internal electron pressure, disperses even before electron-ion collision occurs. Now an increase in T_0 is accompanied by a decrease in T_{im}.

32

With assigned initial temperature T_0 the highest attainable ion temperature depends upon the product $n_0 x_0$ (see Fig. 10). If for each $n_0 x_0$ = const we define T^*_0 as the temperature at which curve $T_{1m}(T_0)$ achieves maximum T^*_{1m}, then we obtain $T^*_e \sim (\bar{n}_e x_0)^{1/4}$. Temperature T^*_0 weakly depends upon ion mass (as $M^{1/4}$) and more strongly depends upon Z. At n_e = const temperature $T^*_e \sim Z^{3/4}$. This is connected basically with the relaxation term since $\tau_{ei} \sim Z^{-2}$. Therefore, we find that when heating lithium deuteride, the ions of lithium are first heated and then, from them, thermal energy is transferred to the deuterons.

Thus, in confined plasma ($n_0 x_0$ = const) it is not possible to obtain ion temperature higher than a certain maximum T^*_{1m}. Moreover, transitions to T^*_0 lead to a drop in ion temperature. However, if with an increase in T_0 we increase $n_0 x_0$, then a further rise in T_1 becomes possible. Precisely this situation can arise under the effect of very powerful pulses on a thick target. An increase in the number of heated particles in this case occurs because of thermal conductivity. Thermal conductivity emerges not as a useless process leading to undesirable losses, but as a mechanism which facilitates the obtaining of high ion temperatures. The heating of ions during electron thermal conductivity is examined in reference [21].

5. From the experimental results discussed above it follows that $n_0 x_0$ = $(1-2) \cdot 10^{19}$ cm^{-2}. With the aid of these measurements, it is possible to explain the neutron yield in the experiments described in reference [1]. If we take $n_0 x_0$ = $2 \cdot 10^{19}$ cm^{-2} and $n_0 \approx 10^{21}$ cm^{-3}, then on the basis of the analytical expressions obtained for the maximally attainable ion temperature we have T_{1m} = T^*_{1m} = 300 eV with an initial electron temperature of $T_0 = T^*_0 \approx 300$ eV. The lifetime of the maximum ion temperature is $\tau_m \approx 5 \cdot 10^{-10}$ s. Hence, according to [18], we obtain for the expected neutron yield $N_m \approx 1$ neutron/pulse, which agrees with the observation in [1] of single neutrons.

33

VI. Conclusion

In the study of plasma heating with ultrashort laser pulses it
was found that the laser pulse, as a rule, is not single but consists
of a whole series of subpulses (peaks) having dissimilar intensity
and distance from each other at different time intervals. The results
obtained with a total laser pulse energy of 0.1 J showed that the
absorption of an individual picosecond pulse occurs when near the
target there is plasma with a concentration lower than critical $n_{\text{кр}}$,
which can be determined from equality $\omega = \omega_p$.

The heating of plasma under the conditions of the conducted
experiments occurs in the following manner. One of the first peaks
hitting the target ionizes it to a depth approximately equal to the
wavelength of the laser emission. After the value of n_e is equalized
with the value of $n_{\text{кр}}$, the rest of the peak is reflected. Simul-
taneously with ionization occurs the heating of plasma to a temperature
of several electron volts. As a result, the plasma formed rather
slowly disperses. All peaks hitting the target in this stage will be
reflected (with the deduction of losses to supplementary ionization)
until particle density falls, as a result of dispersion, to a value
corresponding to $n_{\text{кр}}$. At this time, high-temperature heating of
plasma is possible.

Thus, it is possible to consider established the fact that
reflection of ultrashort pulses occurs in plasma regions where
electron density is near critical. At flux densities used in the
experiments there is no noticeable absorption by the plasma of laser
emission when $\omega_p > \omega$.

The hot plasma formed with initial electron temperature $T_0 \approx 200$
eV, electron density $n_0 = 5 \cdot 10^{20} - 10^{21}$ cm^{-3}, and characteristic
dimension $x_0 = (1-2) \cdot 10^{-2}$ cm during a certain period of time is
nontransparent and the incident peaks are absorbed in it. After the
onset of transparency due to the drop in plasma density during free
expansion, laser emission again penetrates to the surface of the tar-
get and high-temperature heating of a new portion of the substance

34

occurs. The stage of slow dispersion is absent, which indicates the existence near the target of neutral gas or cold plasma with $n < n_{\text{кр}}$.

Theoretical analysis of the possibilities of heating ions in the approach of a uniformly expanding plasma, taking into account electron-ion relaxation and energy loss on emission, indicates that with the prescribed initial conditions n_0, x_0, T_0, ion temperature T_i as a function of time has maximum T_{im}. The dependence of T_{im} on initial data has been obtained. At $n_0 x_0 = $ const quantity T_{im} first increases with an increase in T_0 and after achieving a certain value for T^*_{im}, begins to fall. This drop is explained by two factors.

With an increase in initial electron temperature the rate of electron-ion relaxation decreases in proportion to $T^{-3/2}$. Furthermore, there occurs a simultaneous increase in the dispersion rate (proportional to $T^{1/2}$) and, consequently, a reduction in the time of energy exchange during collisions between electrons and ions.

Thus, in plasma with a fixed number of particles ($n_0 x_0 = $ const) it is not possible to achieve an ion temperature higher than $T^*_{im} \sim (n_o x_o)^{1/3}$. It is possible to achieve a further rise in T_i if we use a thick target and laser energy with which an increase in the number of heated particles because of electronic thermal conductivity becomes noticeable. Thermal conductivity will play not its usual role of energy losses but that of a useful mechanism favorable to the achievement of high ion temperatures with high plasma density [21].

Since the collection of ion energy during relaxation and the emission of the plasma occurs as a result of the same electron-ion collisions and differs only in the size of the cross section, there exists a profound connection between ion temperature and the radiant characteristics of plasma when it is heated by ultrashort laser pulses. It has been shown that T_{im} and the radiant energy are fully determined by the same parameters: T_0 and $n_0 x_0$. Therefore, the diagnostics of the plasma created with ultrashort pulses, with respect to its emission, can be used to determine ion temperature. When radiative losses are small as compared with the total energy of the

plasma (and precisely this usually occurs), the integral radiant energy is proportional to quantity $(n_0 x_0)^2$ and not dependent upon T_0.

On the contrary, pulse duration of the plasma emission $\tau_{изл}$ is determined only by initial temperature T_0 ($\tau_{изл} \sim T_0^{-1/2}$) and does not depend upon $n_0 x_0$. With respect to order of magnitude, $\tau_{изл}$ is fractions of a nanosecond and cannot as yet be measured by existing apparatuses. X-ray pulses from the investigated plasma are, apparently, the shortest that can be obtained today.

The results of this work make it possible to explain experiments in the observation of neutron emission [1]. The neutron yield observed corresponds to $T_0 \approx 900$ eV, $T_1 \approx 300$ eV, $n_0 x_0 = 2\cdot10^{19}$ cm^{-2} when initial electron density n_0 is near critical.

Upon focusing powerful ultrashort pulses the pressure of laser emission near the target can reach high values. However, from the calculations made it follows that the supplementary pulse acquired by the plasma in this case is small as compared with thermal in the ratio v/c where $v \sim \sqrt{T_e}$ is the asymptotic dispersion rate.

Bibliography

1. Басов Н. Г., Захаров С. Д., Крюков П. Г., Сенатский Ю. В., Чекалин С. В. «Письма в ЖЭТФ», 1968, т. 8, № 1, стр. 26.
2. Басов Н. Г., Захаров С. Д., Крохин О. Н., Крюков П. Г., Сенатский Ю. В., Чекалин С. В. Доклад на II Международной конференции по лазерной технике. Вашингтон, 26—28 мая 1969 г.
3. Gobeli G. W., Bushnell J G, Percy P S., Jones E. D. Phys. Rev., 1969, v. 188, № 1, p 300.
4. Floux F., Cognard D, Bobin J. L., Delobeau F., Fauquignon C. C. R. Acad Sc Paris, 1969, v 209, № 15, p. 697.
5. Basov N G. et al. Phenomena in ionized gases Bucharest, 1969.
6. Малютин А А, Щелев М. Я «Письма в ЖЭТФ», 1969, т. 9, № 8, стр. 445.
7. Basov N., Krokhin O, Sklizkov G. IEEE J. Quant. Electr., 1968, v. QE-4, № 1, p 12.
8. Korobkin V. V., Maljutin A A., Schelev M. Ia. J Photographic Sci., 1969, v. 17 № 5, p. 179
9. Басов Н. Г, Бойко В. А., Грибков В. А., Захаров С. М., Крохин О. Н., Склизков Г В «Письма в ЖЭТФ», 1969, т 9, № 9. стр. 520.

10. Jahoda F. C., Little E. M., Quinn W. E., Sawyer G. W., Stratton T. F. Phys. Rev., 1960, v. 119, № 3, p. 843.
Elton R. S., Kolth N. V. Appl. Opt., 1967, v. 6, № 12, p. 2071.
11. «Диагностика плазмы». Под ред. Р. Хаддстоуна и С. Леонарда. Изд-во «Мир», 1967.
12. Матвеев В. В., Соколов А. Д. Фотоумножители в сцинтилляционных счетчиках. Атомиздат, 1962.
13. Спитцер Л. Физика полностью ионизованного газа. Пер. под ред. М. Л. Левина. Изд-во «Мир», 1965.
14. Зельдович Я. Б., Райзер Ю. П. Физика ударных волн и высокотемпературных гидродинамических явлений. Изд-во «Наука». 1966.
15. Weichel H., David C. D., Avizonis P. Appl. Phys. Lett., 1968, v. 11, № 13, p. 376.
16. Коган В. И. В сб. «Физика плазмы и проблема управляемых термоядерных реакций», т. I, стр. 130. Изд-во АН СССР, 1958.
17. Брагинский С. И. В сб. «Вопросы теории плазмы». Атомиздат, 1963, № 1, стр. 183.
18. Арцимович Л. А. Управляемые термоядерные реакции. Физматгиз, 1961.
19. Гинзбург В. Л. «Труды ФИАН СССР им. П. Н. Лебедева», 1962, т. 18, стр. 55.
20. Захаров С. Д., Крохин О. Н., Крюков П. Г., Тюрин Е. Л. «Письма в ЖЭТФ», 1970, т. 12, № 3, стр. 115.
21. Захаров С. Д., Крохин С. п., Крюков П. Г., Тюрин Е. Л. «Письма в ЖЭТФ», 1970, т. 12, № 2, стр. 47.

QUANTUM ELECTRONICS

Collection of Articles

Contents

Translation of Content Titles

1. A study of plasma formed by ultrashort laser pulses.

2. Stimulated emission in the vacuum ultraviolet region.

3. The formation of powerful pulses with a steep leading edge in a laser system with passive nonlinear elements.

4. Power resonances and frequency stabilization of a gas laser with a nonlinearly absorbing cell.

5. A gas laser with nonlinear absorption in the quasi-travelling wave mode.

6. Scattering of coherent light in a cylindrical electron beam.

7. Increasing the brightness of radiation with the aid of a Brillouin laser.

8. Holographic memory devices with information recording by blocks.

9. Methods for selecting types of oscillations in pulse injection lasers.

10. Calculating the effectiveness of a laser with high losses on radiation.

11. Three-dimensional coherent radiation of a ruby laser with pulse quality.

12. A study of the generation of a ruby laser with automatic Q-modulation.

13. The effectiveness of the generation of high-order optical harmonics and multiquanta processes in the field of multimode radiation.

14. The generation of optical harmonics in pulse mode with high pulse repetition frequency.

15. A study of the system of beam deflection in lithium niobete crystals.

16. The optical absorption spectrum of excited ions Cr^{3+} in $MgAl_2O_4$ spinel.

17. Short reviews.

18. Obtaining 1 MW pulses with the free generation of a ruby laser.

19. A single-mode ruby laser with a ring-type resonator.

20. Spatial energy characteristics of fluid circulation for a $POCl_3SnCl_4Nd$ laser.

21. Diffraction effectiveness of a phase hologram formed by a deformation surface.

22. Multiple recording of holograms with extended source of reference beam.

23. Recording holograms on photopolymers.

24. The longitudinal electro-optical effect in sloping sections of lithium niobate.

25. Two-coordinate deflection of light by a Bragg ultrasonic cell.

26. Visualization of objects illuminated by 10.6 μm longwave radiation.

40

ARTICLES TO BE PUBLISHED IN THE THIRD ISSUE OF QUANTUM ELECTRONICS

Translation of Titles

1. The effect of admixture concentration on the threshold characteristics of semiconductor lasers.

2. Laser optron.

3. Characteristics of a gallium arsenide laser with high-energy electron beam pumping.

4. Unlimited extension with distributed radiative losses.

5. Waveguide transmission of videoinformation in coherent light.

6. Vortex discharge as a source of continuous laser pumping.

7. Photoionization of internal electrons in atoms as a method of creating population inversion.

8. Surface disruption stage of a transparent dielectric during laser irradiation.

9. Four-photon parametric frequency selection within wide lines of stimulated radiation.

10. Edge effects on the properties of unstable resonators.

11. In addition, a number of short reviews will be published, including:

12. Oscillation temperatures in carbon dioxide lasers.

13. Widening the spectrum of laser radiation by brightening a nonlinear filter.

14. Contrast power resonances in a helium-neon laser with an absorbing cell.

15. A laser with Q-switching for high-speed photography.

16. A study on the Faraday effect in indium antimonide at wavelengths of 10.6 μm.

17. Relationship of pumping conditions for a garnet pulsed laser with tube filling.

COMMENTS OF EDITORIAL STAFF

Quantum electronics, whose emergence is connected with the first molecular generator on an ammonium beam, presently occupies a completely independent area of physics.

An unusually large group of scientists and engineers is working both on the overall problem of the interaction of coherent electromagnetic radiation (primarily light) with matter and on the different applications of the common principles in specific instruments. International and national conferences on quantum electronics are completely comparable to conferences and congresses on traditional areas of physics. A considerable number of specialized forms, closely connected with quantum electronics, have been held: conferences on nonlinear optics and holography, on the interaction of radiation with matter, etc. This is completely natural for such a strongly developing area of knowledge.

The works of this group of physicists and engineers on quantum electronics can and should be combined on the pages of a specialized periodical. "Quantum Electronics," published by the Sovetskoye Radio Publishing House, serves this purpose.

In 1971 the collection will be published periodically; we hope that in the near future it will become a journal.

The editorial staff of "Quantum Electronics" accepts for publication original articles and short reports. In each issue there will be one review article on the present problems in quantum electronics.

The electoral staff assumes that the subjects in the collection will be sufficiently broad. Works connected with the applications of lasers in science and technology, as well as those describing specific devices, will be accepted.

Thus, we hope to be able to concentrate efforts in quantum electronics in one publication which, undoubtedly, will effect an improvement in the quality of published works, an increase in the volume of information, and, on the whole, further progress in quantum electronics.